Journal of Alloys and Compounds 506 (2010) 815–819

Contents lists available at ScienceDirect

Journal of Alloys and Compounds

journal homepage: www.elsevier.com/locate/jallcom

# Multiferroic properties of $BiFeO_3$ doped $Bi(MgTi)O_3$–$PbTiO_3$ ceramic system

Radheshyam Rai [a,*], Andrei L. Kholkin [a], Seema Sharma [b]

[a] Department of Ceramics and Glass Engineering and CICECO, University of Aveiro, 3810-193 Aveiro, Portugal
[b] School of Materials, Materials Science Center, University of Manchester, Manchester M1 7HS, UK

ARTICLE INFO

*Article history:*
Received 17 May 2010
Received in revised form 7 July 2010
Accepted 8 July 2010
Available online 16 July 2010

*Keywords:*
Ceramics
Magnetic materials
Materials science
Perovskites

ABSTRACT

Ceramic samples of $[BiFeO_3]_y(BiMg_{0.5}Ti_{0.5}O_3)_{1-y}]_{0.55}[PbTiO_3]_{0.45}$ designated as (BF–BMT–PT) were prepared by high temperature solid-state reaction method. X-ray diffraction analysis of the powder samples suggests the formation of a single-phase material with transformation from rhombohedral to tetragonal crystal structure with increase in BF content. Polarization vs electric field ($P$–$E$) hysteresis studies show maximum remanent polarization ($P_r \sim 1.4\ \mu C/cm^2$) for composition $y = 0.08$. Dielectric studies of the compounds as a function of temperature at frequency 100 kHz show that the compounds undergo a diffuse phase transition with a transition temperature increasing with increasing $y$. The diffusivity parameter of the phase transition for these compounds yielded values between 1.6 and 1.8 indicating significant variation of degree of disordering in the system.



## 1. Introduction

Perovskite solid solutions have been an active area of research due to their importance in ferroelectric, ferromagnetic and piezoelectric applications along with their fascinating physical properties, [1–6]. In particular, Bi-based ferroelectrics are under intense investigation, because they exhibit both large polarization [7–9] and multiferroic behavior [10,11]. The coexistence of magnetic and electric subsystems endows materials with the "product" property, thus allowing an additional degree of freedom in the properties of actuators, sensors, and storage devices [12–17]. However, the choice of single-phase materials exhibiting coexistence of strong ferro-ferrimagnetism (FM) and ferroelectricity (FE) is limited [18]. Therefore, multiferroic composites comprised of a mixture of two or three different types of materials with separate or combined ferromagnetic and ferroelectric properties have been proposed. These composites could be in the form of multilayers or nanocomposites.

$BiFeO_3$ (BF), with a rhombohedrally distorted perovskite structure space group $R3c$, is the only known perovskite oxide that exhibits both antiferromagnetism weak magnetism from canted spins or parasitic ferromagnetism and ferroelectricity at room temperature. This material has recently attracted significant attention from the viewpoint of both fundamental research and the potential for practical applications involving mutual control of magnetization and polarization. Nevertheless, it has a serious electrical leakage problem, most likely as a result of defects and nonstoichiometry. Recently for high temperature applications, new piezoelectric ceramics of the general formula $(1-x)BiMeO_3$–$xPbTiO_3$ ($Me^{3+}$ = Sc, In, Y, Yb, Fe, Ga, etc.) with paraelectric–ferroelectric phase transition temperature higher than lead zirconate titanate (PZT) and its contemporary compositions have been reported [5,19–21]. Alternative lower cost systems, for example $BiFeO_3$–$PbTiO_3$ and $BiGaO_3$–$PbTiO_3$ have been investigated by other researchers in order to identify particular compositions that merit further development for use in high temperature piezoelectric devices [22–25]. Some of these reports have been concerned with the use of bismuth based complex perovskites, including $Bi(Mg_{0.5}Ti_{0.5})O_3$ (BMT) and $Bi(Mg_{0.5}Zr_{0.5})O_3$ (BMZ) [6,8,9,26–29]. BMT–PT system in particular has shown significant promise with respect to a relatively high Curie temperature ($T_c \sim 450\ ^\circ C$) and high remanent polarisation ($P_r \sim 0.38\ C\ m^{-2}$) [26]. Early studies on perovskite-structured $Bi(Me)O_3$–$PbTiO_3$ solid solutions were mostly concerned with compounds containing transition metal Me ions such as $Fe^{3+}$ and $Mn^{3+}$ [30,31]. These materials show high temperature ferroelectric–paraelectric phase transitions but the piezoelectric and dielectric properties were limited or unknown due to their high electrical conductivity. In this research report, an attempt has been made to study the ternary system $BiFeO_3$–$BiMgTiO_3$–$PbTiO_3$ (BF–BMT–PT) aiming at the development of high dielectric constant multiferroic (magnetoelectric) materials with reduction in electrical leakage current.

## 2. Experimental procedures

Polycrystalline samples of $[(BiFeO_3)_y(BiMg_{0.5}Ti_{0.5}O_3)_{1-y}]_{0.55}[PbTiO_3]_{0.45}$, where ($y$ = 0.025, 0.05, 0.07, and 0.08), were synthesized from high purity oxides of $Bi_2O_3$, $Fe_2O_3$, $TiO_2$, MgO, and PbO (99.9% M/S Aldrich Chemicals) using high temperature

* Corresponding author. Tel.: +351 962782932; fax: +351 234425300.
*E-mail address:* radheshyamrai@ua.pt (R. Rai).

0925-8388/$ – see front matter © 2010 Elsevier B.V. All rights reserved.
doi:10.1016/j.jallcom.2010.07.080

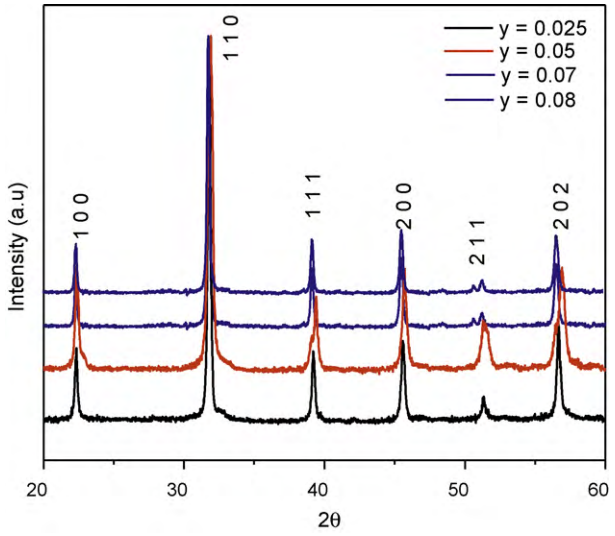


**Fig. 1.** X-ray powder diffraction patterns of the BF–BMT–PT ceramics for different compositions.

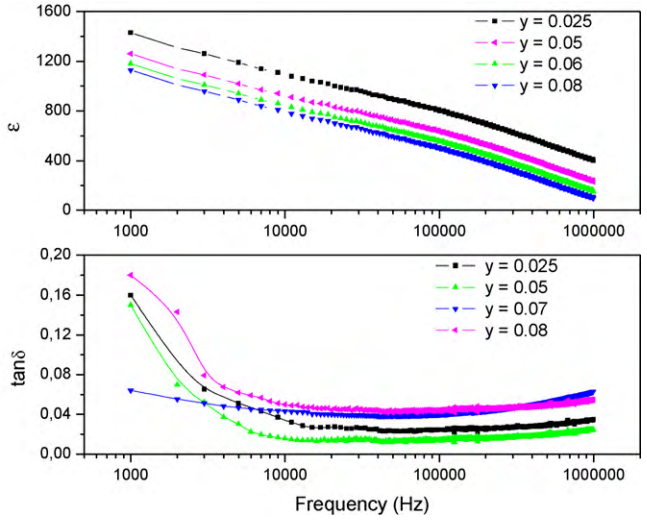


**Fig. 2.** Variation of dielectric constant of BF–BMT–PT as a function of frequency at room temperature.

solid-state reaction technique in an ambient atmosphere. The constituent compounds in suitable stoichiometry were thoroughly mixed in a ball milling unit for 24 h. The calcined fine powder was cold pressed into cylindrical pellets of 10 mm in diameter and 1–2 mm in thickness using a hydraulic press at a pressure of $6 \times 10^7$ kg m$^{-2}$. These pellets were sintered at 1050 °C for 4 h in air. The formation and quality of compounds were verified by X-ray diffraction (XRD) technique. The XRD pattern of the compounds was recorded at room temperature using X-ray powder diffractometer (Rigaku Minifiex Japan) with Cu Kα radiation (λ = 1.5418 Å) in a wide range of Bragg angles $2\theta$ ($20° \leq 2\theta \leq 60°$) at a scanning rate of 2 min$^{-1}$. The dielectric constant ($\varepsilon$) and loss tangent ($\tan\delta$) of the compounds were measured using a 4192A LF Impedance Analyser (HP) as a function of frequency at room temperature (RT) and temperature (RT to 500 °C) at different frequencies with a laboratory made experimental setup. Ferroelectric hysteresis was measured by using Radiant Technologies, Precision High Voltage Interface Trek MODEL 609B at room temperature. The magnetic data was recorded with the help of vibrating sample magnetometer (VSM) (Cryogenic).

## 3. Results and discussion

The narrow and symmetric X-ray diffraction peaks of the BF–BMT–PT compounds indicate homogeneity and good crystallization of the samples. Room temperature XRD patterns of the BF–BMT–PT perovskite type ceramics are plotted in Fig. 1. All the reflection peaks were indexed using observed inter-planar spacing $d$, and lattice parameters of BF–BMT–PT were determined using a least-squares refinement method. A good agreement between calculated and observed $d$ values of all diffraction lines (reflections) of BF–BMT–PT system with different y content suggests that there is a change in the basic crystal structure from rhombohedral to tetragonal. Crystal tetragonality ($c/a$) (Table 1) is found to increase with increase in BF content resulting in hard and denser ceramics.

Fig. 2 shows variation of $\varepsilon$ with frequency at room temperature for all compositions. It was found that with the increase of frequency $\varepsilon$ decreases following the logarithmic law. This type of relaxation could be related to the domain wall propagation in a random media similar to that in magnetic systems. The same type of frequency dependence is found in many ferroelectric ceramics [32,33]. Room temperature variation of dielectric loss with frequency shows an appreciable change in low frequency but at higher frequency it does not show an appreciable change. In BF–BMT–PT ceramics, the dielectric permittivity decreases with increasing BF content. The larger values of $\varepsilon$ at room temperature and lower frequency dispersion in BF–BMT–PT may also be ascribed due to the interfacial and dipolar contribution of polarization [34]. The fall in dielectric permittivity arises from the fact that polarization does not occur instantaneously with the application of the electric field because of inertia. The delay in response towards the impressed alternating electric field leads to loss and decline in dielectric constant [35]. At low frequencies, all the polarizations contribute and as the frequency is increased, those with large relaxation times cease to respond and hence results in the decrease of the dielectric permittivity.

Fig. 3(a) and (b) shows the variation of $\varepsilon$ and $\tan\delta$ of BF–BMT–PT with temperature at 10 kHz frequency. Here, the dielectric permitivity increases gradually with an increase in temperature up to transition temperature ($T_c$) and then decreases. The region around the dielectric peak is apparently broadened. The broadening or diffuseness of peak occurs mainly due to compositional fluctuation and/or substitution disordering in the arrangement of cations in one or more crystallographic sites of the BF–BMT–PT structure. The value of peak dielectric permitivity ($\varepsilon_{max}$) increases initially with the increase of concentration (Table 2). It reveals a maximum at about 510 °C. Above this temperature the dielectric permittivity and loss decreases till 570 °C and then begins to increase. Such type of behavior was also observed in BMT–PT system [36] by Sharma et al., which was attributed to the space charge polarization at high temperatures. With the increase in BF content, the increase in Curie temperature and dielectric parameters at 100 kHz are shown in Fig. 3(c).

**Table 1**
Structural data for different compositions of BF–BMT–PT.

| Samples | Structure | $a$ (Å) | $c$ (Å) | $c/a$ | Measured density ((g m)/cm$^3$) |
|---|---|---|---|---|---|
| $y = 0.025$ | Rhombohedral | 5.0260 | – | | 8.31 |
| $y = 0.05$ | Rhombohedral | 5.0434 | – | | 8.35 |
| $y = 0.07$ | Tetragonal | 3.5652 | 4.0542 | 1.13 | 8.55 |
| $y = 0.08$ | Tetragonal | 3.5523 | 4.6106 | 1.29 | 8.68 |

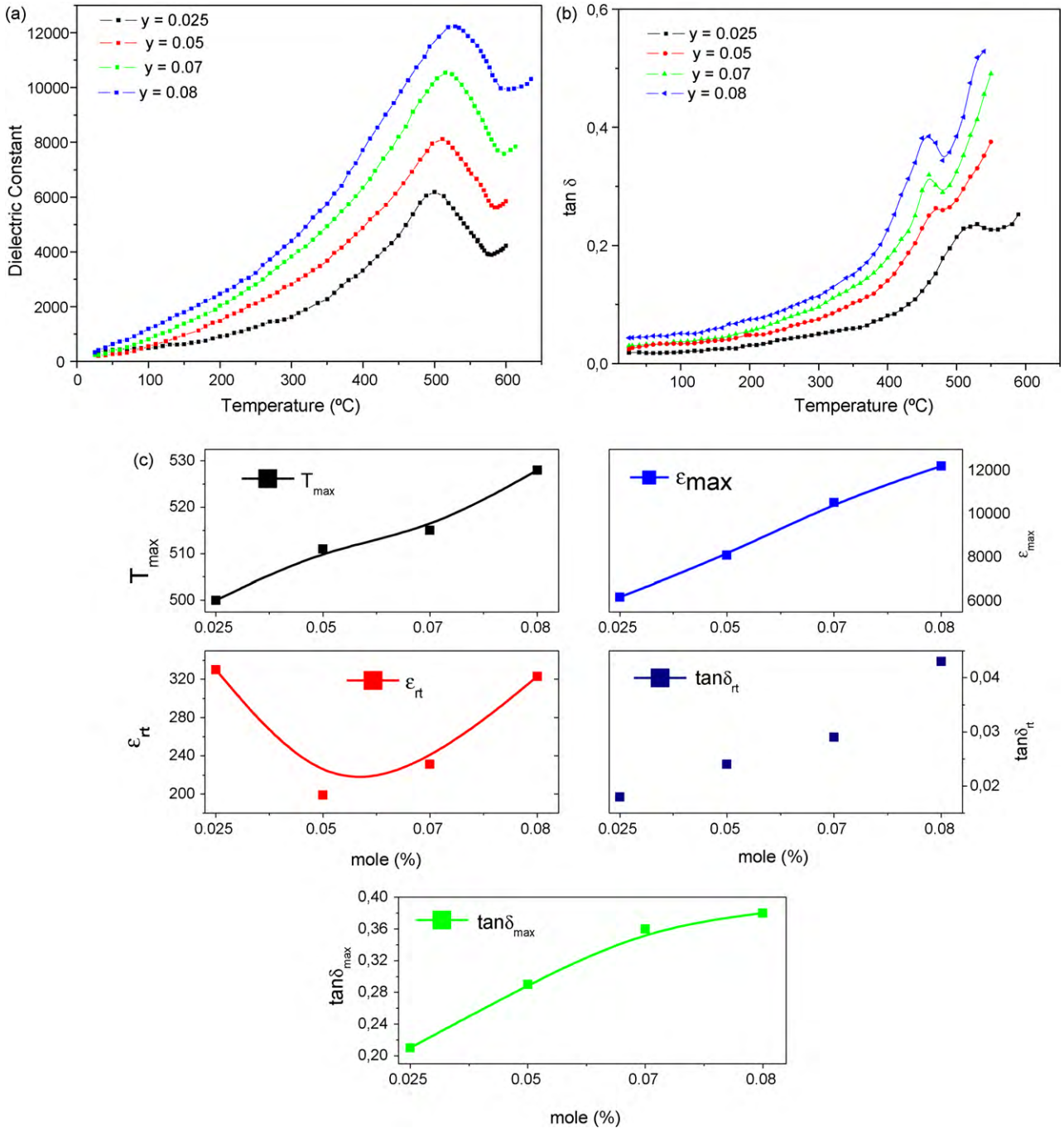


**Fig. 3.** (a) Variation of dielectric constant, (b) variation of dielectric loss of BF–BMT–PT as a function of temperature at 100 kHz respectively and (c) $T_{max}$, $\varepsilon_{max}$, $\varepsilon_{rt}$, tan $\delta_{rt}$ and tan $\delta_{max}$ vs doping concentration (mol%) at 100 kHz respectively.

**Table 2**
Some physical parameters for different compositions of BF–BMT–PT.

| Physical parameters | $y = 0.025$ | $y = 0.05$ | $y = 0.07$ | $y = 0.08$ |
|---|---|---|---|---|
| $\varepsilon_{rt}$ | 330 | 199 | 231 | 323 |
| tan $\delta_{rt}$ | 0.018 | 0.024 | 0.029 | 0.043 |
| $T_c$ | 500 | 511 | 515 | 528 |
| $\varepsilon_{max}$ | 6185 | 8114 | 10,541 | 12,229 |
| tan $\delta_{max}$ | 0.21 | 0.29 | 0.36 | 0.38 |
| $\gamma$ | 1.60 | 1.70 | 1.75 | 1.8 |

We have also made attempts to measure the induced polarization electric field ($P$–$E$) hysteresis loop at room temperature (Fig. 4). No saturation in polarization–electric field ($P$–$E$) curve could be obtained for the ceramic samples, up to a maximum of 8 kV/mm applied electric field. This is due to the increase in the BF content which hardens the material. Because of the hardening effect of the BF content, the domain switching becomes more and more difficult. This type of effect was also observed in BF doped $Bi(Mg_{0.5}Zr_{0.5})O_3$–$PbTiO_3$ ceramic system [30]. The observed coercive filed for $y = 0.08$ is $E_c \sim 70$ kV/cm and the maximum remanent polarization is $P_r \sim 1.4\ \mu C/cm^2$.

In BF–BMT–PT, Fe magnetic moments are coupled ferromagnetically within the pseudocubic (1 1 1) plane and antiferromag-

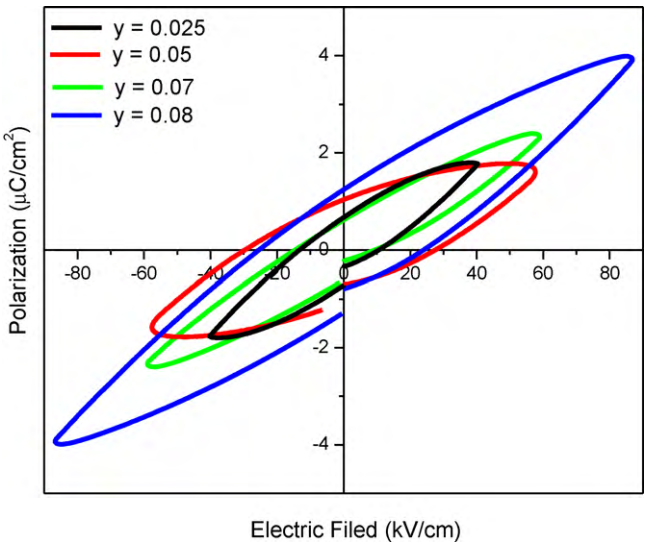


**Fig. 4.** *P–E* hystersis loops for BF–BMT–PT ceramics at room temperature.

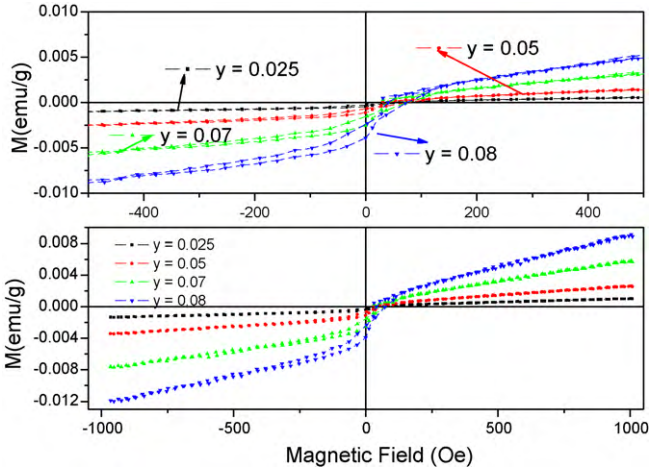


**Fig. 5.** Magnetization vs magnetic field curves for BF–BMT–PT samples at room temperature.

netically between the adjacent planes. There is a canting of antiferromagnetic sublattices resulting in a macroscopic magnetization. Superimposed on antiferromagnetic ordering, there is a spiral spin structure which leads to cancellation of macroscopic magnetization. Magnetization is induced in the sample whenever this spiral structure is suppressed [37]. All the samples show unsaturated magnetization loops (Fig. 5) which confirm the basic antiferromagnetic nature of the compounds. The magnetization increases with the increase in content of BF. The magnetization is higher, when the concentration of BF is increased from 0.025 to 0.08. This could be due to the structural distortion in the perovskite i.e., the canted spin arrangement of unpaired electrons on $Fe^{3+}$ ions is caused by incorporating $Pb^{2+}$ ions to A sites and/or $Ti^{4+}$ ions to B sites of the perovskite structure of $BiFeO_3$. This structural distortion could lead to the suppression of the spin spiral and hence enhance the magnetization in the system.

The quantitative assessment of the diffusivity ($\gamma$) of the broadened peaks in the paraelectric phase was evaluated using the

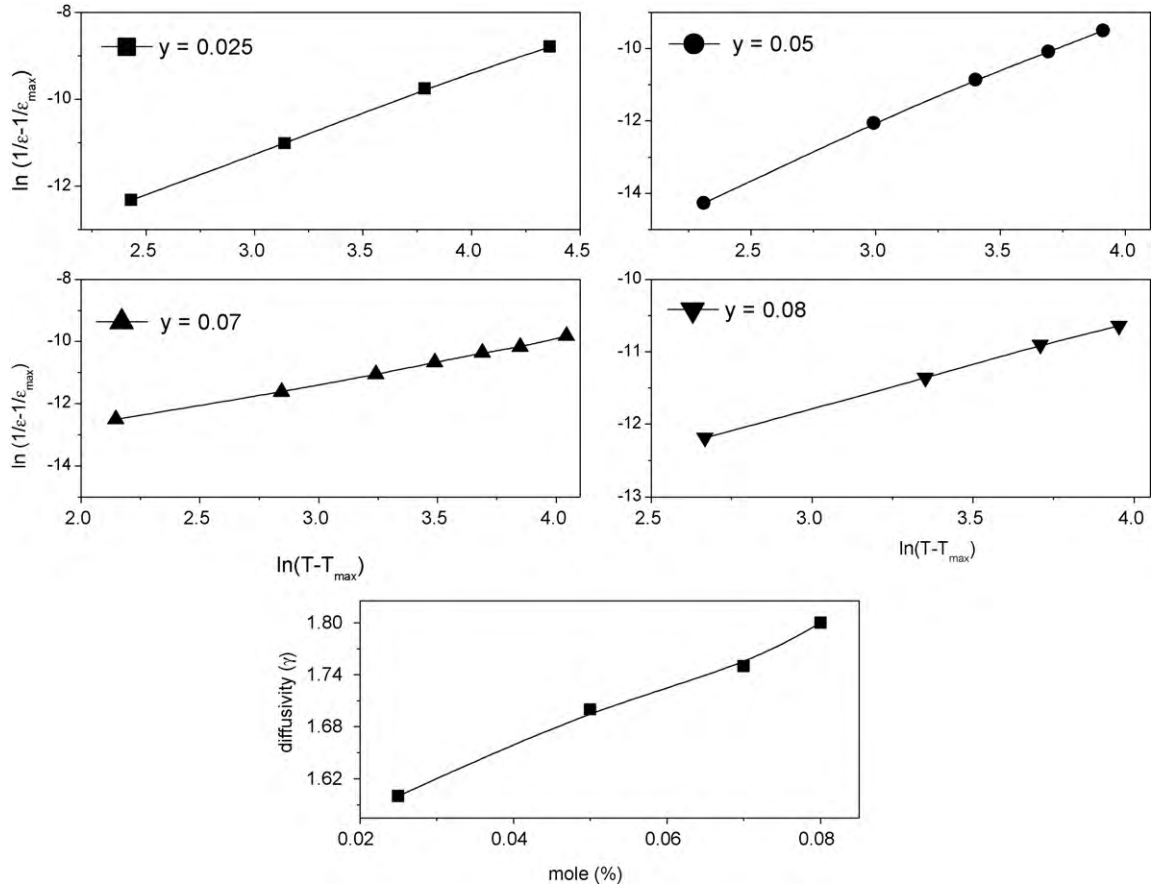


**Fig. 6.** Variation of $\ln(1/\varepsilon - 1/\varepsilon_{max})$ vs $\ln(T - T_{max})$ in the paraelectric region at 100 kHz.

expression $\ln(1/\varepsilon - 1/\varepsilon_{max})$ vs $(T - T_c)^{\gamma}$ [38]. The plot (Fig. 6) of $\ln(1/\varepsilon - 1/\varepsilon_{max})$ vs $\ln(T - T_{max})$ for all compositions was extracted from the plot by fitting a straight-line equation. The value of $\gamma$ was found to be between 1 (normal Curie Weiss behavior) and 2 (completely disordered), which further confirmed the diffuse phase transition in the materials. The double logarithmic relationship between $(1/\varepsilon - 1/\varepsilon_{max})$ and $(T - T_{max})$, unequivocally displays linear behavior in the temperature range between $T_{max}$ and $T_{cw}$. The values of $\gamma$ fall into $1.6 < \gamma < 1.8$. For the comparative purpose, the plots of diffusivity against concentration at 100 kHz for various compositions are shown in Fig. 6 as an inset figure.

## 4. Conclusions

BF–BMT–PT solid solution ceramics in single phase were prepared using high temperature solid-state reaction method. The crystal structure transforms from rhombohedral to tetragonal with increase in BF content. $BiFeO_3$ doping in BMT–PT exhibits many interesting features, such as shift in transition temperature, diffuse phase transition and enhanced magnetic properties. The magnetization increases with the increase in BF content in the solid solution. Polarization–electric field hysteresis curves show decrease in the remanent polarization with BF content and hardens the material. Because of the hardening effect of the BF content, the domain switching becomes more and more difficult.

## References


[1] R.E. Cohen, Nature 358 (1992) 136.
[2] L. Bellaiche, A. Garcia, D. Vanderbilt, Phys. Rev. Lett. 84 (2000) 5427.
[3] I. Grinberg, V.R. Cooper, A.M. Rappe, Nature 419 (2002) 909.
[4] Y. Saito, H. Takao, T. Tani, T. Nonoyama, K. Takatori, T. Homma, T. Nagaya, M. Nakamura, Nature 432 (2004) 84.
[5] R.E. Eitel, C.A. Randall, T.R. Shrout, P.W. Rehrig, W. Hackenberger, S.E. Park, Jpn. J. Appl. Phys. 40 (2001) 5999.
[6] M.R. Suchomel, P.K. Davies, Appl. Phys. Lett. 86 (2005) 262905.
[7] Y. Uratani, T. Shishidou, F. Ishii, T. Oguchi, Jpn. J. Appl. Phys. 44 (2005) 7130.
[8] M.D. Snel, W.A. Groen, G.D. With, J. Eur. Ceram. Soc. 25 (2005) 3229.
[9] A. Moure, M. Algueró, L. Pardo, E. Ringgaard, A.F. Pedersen, J. Eur. Ceram. Soc. 27 (2007) 237.
[10] J. Wang, J.B. Neaton, H. Zheng, V. Nagarajan, S.B. Ogale, B. Liu, D. Viehland, V. Vaithyanathan, D.G. Schlom, U.V. Waghmare, N.A. Spaldin, K.M. Rabe, M. Wuttig, R. Ramesh, Science 299 (2003) 1719.
[11] A.A. Belik, S. Iikubo, K. Kodama, N. Igawa, S. Shamoto, S. Niitaka, M. Azuma, Y. Shimakawa, M. Takano, F. Izumi, E.T. Muromachi, Chem. Mater. 18 (2006) 798.
[12] T. Goto, T. Kimura, G. Lawes, A.P. Ramirez, Y. Tokura, Phys. Rev. Lett. 92 (2004) 257201.
[13] T. Kimura, T. Goto, H. Shintani, K. Ishizaka, T. Arima, Y. Tokura, Nature 26 (4) (2003) 55.
[14] T. Lottermoser, T. Lonkai, U. Amann, D. Hohlwein, J. Ihringer, M. Fiebig, Nature 430 (2004) 541.
[15] H. Ohno, D. Chiba, F. Matsukura, T. Omiya, E. Abe, T. Dietl, Y. Ohno, K. Ohtani, Nature 408 (2000) 944.
[16] B. Lorenz, Y.Q. Wang, Y.Y. Sun, C.W. Chu, Phys. Rev. B 70 (2004) 212412.
[17] N. Hur, S. Park, P.A. Sharma, J.S. Ahn, S. Guha, S.W. Cheong, Nature 429 (2004) 392.
[18] W. Prellier, M.P. Singh, P. Murugavel, J. Phys.: Condens. Matter 17 (2005) R803.
[19] R.E. Eitel, C.A. Randall, T.R. Shrout, S.E. Park, Jpn. J. Appl. Phys. 41 (2002) 2099.
[20] Y. Horibe, M. Nakayama, Y. Hosokoshi, T. Asaka, Y. Matsui, T. Asada, Y. Koyama, S. Mori, Jpn. J. Appl. Phys. 44 (2005) 7148.
[21] I. Sterianou, I.M. Reaney, D.C. Sinclair, D.I. Woodward, D.A. Hall, A.J. Bell, T.P. Comyn, Appl. Phys. Lett. 87 (2005) 242901.
[22] D.I. Woodward, I.M. Reaney, R.E. Eitel, C.A. Randall, J. Appl. Phys. 94 (2003) 3313.
[23] J.R. Cheng, W. Zhu, N. Li, L.E. Cross, Mater. Lett. 57 (2003) 2090.
[24] J.R. Cheng, N. Li, L.E. Cross, J. Appl. Phys. 94 (2003) 5153.
[25] X. Zheng, Q. Xua, Z. Wen, X. Lang, D. Wu, T. Qiu, M.X. Xu, J. Alloys Compd. 499 (2010) 108–112.
[26] C.A. Randall, R.E. Eitel, B. Jones, T.R. Shrout, D.I. Woodward, I.M. Reaney, J. Appl. Phys. 95 (2004) 3633.
[27] M.R. Suchomel, P.K. Davies, J. Appl. Phys. 96 (2004) 4405.
[28] D. Lina, K.W. Kwok, H.L.W. Chan, J. Alloys Compd. 481 (2009) 310–315.
[29] Q. Xua, H. Zai, D. Wu, Y.K. Tang, M.X. Xu, J. Alloys Compd. 485 (2009) 13–16.
[30] S. Sharma, D.A. Hall, A. Sinha, Mater. Res. Bull. 44 (2009) 1405.
[31] R. Rai, A. Kholkin, S. Pandey, N.K. Singh, J. Alloys Compd. 488 (2010) 459.
[32] R. Rai, A. Sinha, S. Sharma, N.K.P. Sinha, J. Alloys Compd. 486 (2009) 273–277.
[33] R. Rai, I. Bdikin, M.A. Valente, A.L. Kholkin, Mater. Chem. Phys. 119 (2010) 539.
[34] K.V. Rao, A. Smakula, J. Appl. Sci. 37 (1966) 319.
[35] S. Sharma, D.A. Hall, P.S. Mulage, Mater. Lett. 61 (2007) 3352.
[36] S. Sharma, D.A. Hall, J. Electroceram. 20 (2008) 81.
[37] C. Ederer, N.A. Spaldin, Phys. Rev. B 71 (2005), 060401(R).
[38] M.S. Pilgrim, A.E. Sutherland, R. Winzer, J. Am. Ceram. Soc. 73 (1990) 3122.